

Cassiterite U-Pb isotope age of tin ore North Langsong deposit Tanky area, Nghean, Vietnam

NGUYEN Van Dat^{1*}, LE Canh Tuan², TRINH Hai Son¹, NGUYEN Tien Quang¹, NGUYEN Quang Minh³

¹ Viet Nam Institute of Geosciences and Mineral Resources; 67 Chienthang Street, Vanquan, Hadong, Hanoi, Vietnam

² Faculty of Geology, Hanoi University of Natural Resources and Environment; 41A Phudien Street, Bactuliem, Hanoi, Vietnam

³ Hanoi University of Mining and Geology; 18 Vien Ward, Dongngac, Bactuliem, Hanoi, Vietnam

* Corresponding email: nguyendatdcak52@gmail.com

Abstract: *The North Langsong tin deposits are located in Tanhop commune, Tanky district, Nghean, and belong to the Phuhoat uplifted structure. This is the biggest tin ore area in the Northern and Central region of Vietnam. Tin accompanies quartz veins in the northeast-southwest fault zone, developed in carbonate rock formations. The main ore components include pyrite, arsenopyrite, cassiterite, and less commonly galena, chalcopyrite, magnetite, and secondary minerals such as limonite, goethite, and psilomelan. Authors used the results of LA-ICP-MS U-Pb cassiterite analysis to interpret the relationship between tin mineralization and granitoid intrusion. U-Pb analysis of cassiterite from the North Langsong tin deposits yielded isotopic ratios of $^{207}\text{Pb}/^{206}\text{Pb}$ - $^{238}\text{U}/^{206}\text{Pb}$ ranging from 0.0000 to 1.2947 and from 0.0049 to 0.3626, with an age of 35.1 ± 5.2 Ma. On that basis, the authors conclude that the North Langsong ore deposits are associated with young (Paleogene) magmatic activity, represented here by granitoid rocks of the Ban Chieng complex.*

Keywords: *Cassiterite U-Pb dating; North Langsong tin deposit; Banchieng granite; Tanty Nghean; Central Vietnam*

1. Introduction

Determination of the age of rocks and ores is essential for studying ore deposits, especially endogenous ones. Geological age plays an important role in determining the origin and temporal relationships between injections of magmatic rocks and the associated hydrothermal mineralization. Today, modern, highly accurate analytical methods are used to determine the age - dating of rocks and ores including: Zircon U-Pb, muscovite $^{40}\text{Ar}/^{39}\text{Ar}$ isotope, sulfide Re-Os, and cassiterite U-Pb (Hieu et al., 2016; Zhang et al., 2014, 2015, 2019b; Bui et al., 2017, 2022; Bai et al., 2013).

Several studies have confirmed that cassiterite is the dominant tin ore mineral in skarn, greisen, pegmatite, and hydrothermal deposits (Taylor, 1979; Lehmann, 1982). These types of deposits are often associated with granite intrusions (Bui et al., 2022; Lehmann, 1982; Taylor, 1979). According to Machado and Simonetti (2001), Li et al (2016), Lin et al (2016), the analytical method of laser ablation inductively coupled plasma mass spectrometry (LA-ICP-MS) provides reliable results for determining the formation age of uranium-bearing minerals such as zircon, monazite, cassiterite, titanite, and rutile and has also been successfully performed in various areas (Gulson and Jones, 1992; Liu et al., 2007; Yuan et al., 2008; Zhang et al., 2014, 2015; Li et al., 2016; Zhang et al., 2017a; Mao et al., 2020; Bui et al., 2022).

Tanky district, located in the northwest of Nghean province, North Central Vietnam, belongs to the uplifted structure of Phuhoat, which has the potential for tin mineralization. There are more than 10 tin mines here. Among them, the North Langsong tin mine in Tanhop commune, Tanky district, Nghean, Vietnam province is one of the main mines. In previous studies, there have been no studies on the age of formation and origin of mineralization.

The research was conducted with the goal of determining the characteristics and age of tin ore formation at the North Langsong mine. Research results help determine the relationship between tin mineralization and magma activity. Thereby determining the origin of ore and assessing the potential of tin ore in the area.

2. Geological setting

2.1. Regional geology

The research area belongs to the Phuhoat uplifted structure, developing in the northeast-southwest direction, extending from Vietnam to Laos. It is controlled by the Songma and Songca fault systems. The northeast borders the Songma suture zone, the southwest borders the Truongson belt, and the southeast borders the Samneua-Hoanhson zone. (Fig. 1a) (Lepvrier et al., 1997; Jolivet et al., 2001; Tran, 2009; Tran et al., 2016). Phuhoat uplifted structure is located in the center of the Truongson orogenic belt, adjacent to the Samneua-Hoanhson zone and the Songma suture zone. This is an important endogenous tectonic and mineralogical belt of Southeast Asia (Lepvrier et al., 1997; Tran et al., 2008; Roger et al., 2012; Liu et al., 2012a). This is a promising place for mineralization such as tin, copper, gold, silver, ruby-sapphire, iron and others (Tran et al., 2009; Kamvong et al., 2014; Zaw et al., 2014; Shi et al., 2015).

Phuhoat uplifted structure has been referred to various names: Tectonic Arc (Fromaget, 1941), Structural-Facial Zone (Dovjikov et al., 1965), Central Massif (Le., 1969), Late Hercynian Fold Zone (Tran et al., 1986), Phuhoat Massif (Lepvrier et al., 1997); Phuhoat uplifted (Tran., 2009) and Late Neoproterozoic-Early Palaeozoic Microcontinent (Tran et al., 2020). The sedimentary and metamorphic rocks in the uplifted structure of the Phuhoat include the Proterozoic, Paleozoic, and Mesozoic formations cut through by the Triassic and Paleogene granites (Jolivet et al., 1999; Le et al., 1994).

These metamorphic sedimentary rocks are divided into five formations including: Bukhang formation (Neoproterozoic; quartz two-mica, plagioclase sillimanite schist, plagioclase-sillimanite schist, biotite-amphibole quartzite, two-mica, garnet-bearing schist, marble lenses), Songca formation (Ordovician-Silurian; quartz-biotitic schist, mica schist, quartzite, sericite schist, sandstone, siltstone, limestone, rhyolite), Lakhe formation (Lower Carboniferous; conglomerate, sandstone, siltstone, siliceous shale, thin-bedded limestone), Bacson formation (Carboniferous; thick-bedded to massive limestone), and Dongtrau formation (Middle Triassic; clastic sediment, tuff sandstone, tuff siltstone, rhyolite, limestone, marl) (Le et al., 1994; Le et al., 2001) (Fig. 2). Intrusion magmatic rocks were mainly formed during the Triassic and late Paleogene-Early Neogene periods, and are widely distributed in the Phuhoat uplifted structure.

The Middle Triassic intrusive rocks have petrographic compositions including biotite granite, biotite-plagioclase granite, granitogneiss (Le et al., 1994; Nagy et al., 2000; Nguyen et al., 2014, 2015; Bui et al., 2017, 2022) (Fig. 1b). The results of absolute age-dating of samples using U-Pb zircon isotope (SHRIMP) methods give an age of 244 ± 7 Ma (Carter et al., 2001) and 249 ± 5 - 240.7 ± 3.1 Ma (Nguyen et al., 2014, 2015), respectively.

The Quyhop-Tanky area is located in the southeast of the Phuhoat uplifted structure. This area has complex geological structures, formed during the Cenozoic period (Jolivet et al., 1999). Developed in the plastic deformation zone along the southwest edge of the Songma suture zone and the Ailaoshan-Red River deep fault zone. Ailaoshan-Red River is a large-scale shear zone, extending northwest-southeast, located east of the Ailaoshan suture zone (Fig. 1a). This is an important structure hosting mineralization of Sn, Mo, Cu, Au formed during the Late Pleogene-Early Neogene period (Bui et al., 2022; Duong et al., 2021).

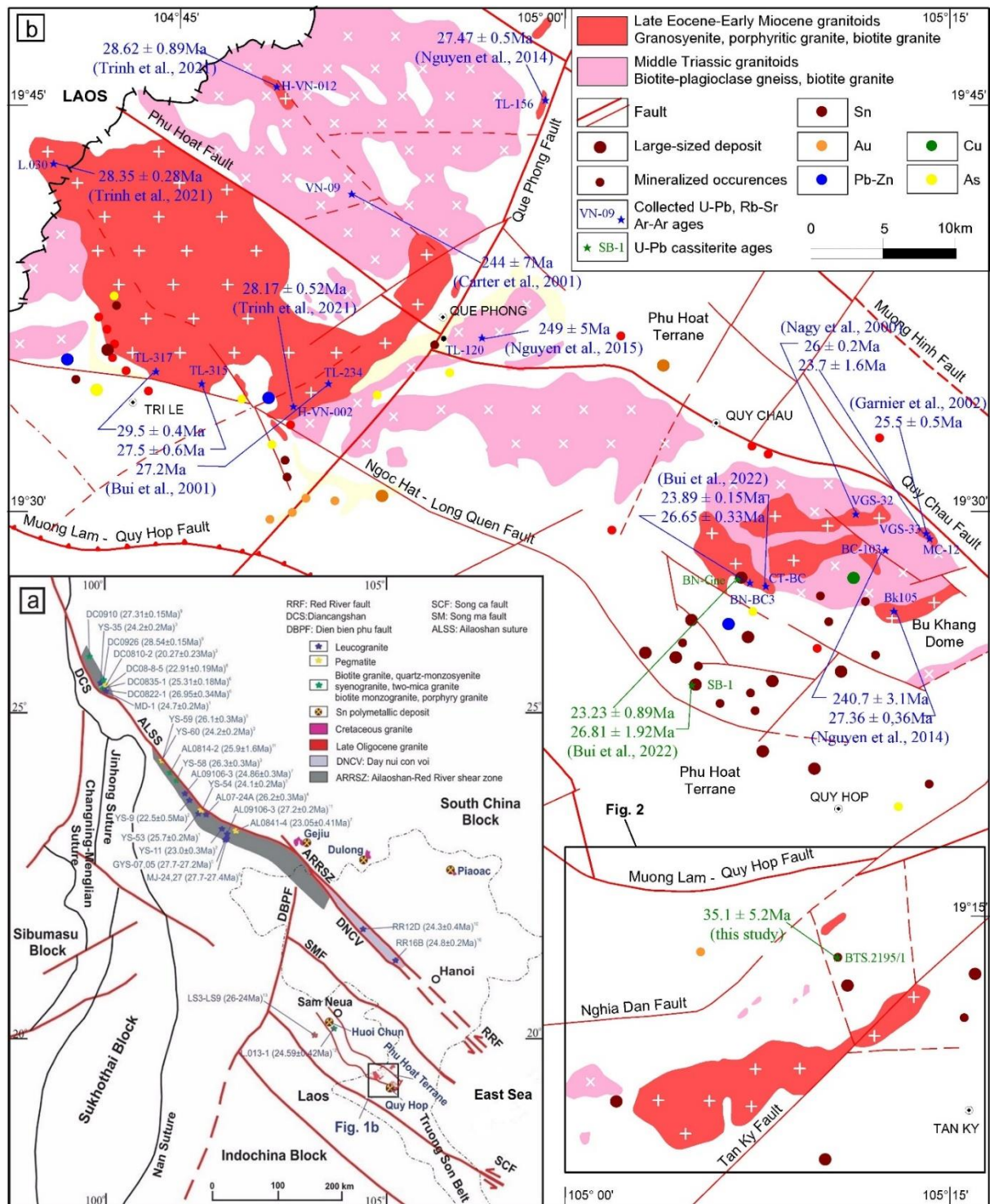


Fig. 1. (a) Tectonic map of Indochina and adjacent areas (Zhang and Schärer., 1999; Tang et al., 2013); (b) Distribution diagram of intrusion magma rocks in Phuhoat uplifted structural (Le et al., 1994; Tri., 2009; Bui et al. 2022). Geological age data according to table 2.

The Banchieng complex has lithological composition built with: biotite granite, porphyritic granite, two mica granite, and granosyenite, forming three main blocks in the Quephong, Quyhop, and Tanky. Isotope age analysis using the zircon U-Pb ages of 26.0-23.7 Ma (Nagy et al., 2000); whole-rock Rb-Sr isochron ages of 27±1 Ma, and biotite K-Ar isochron ages of 24.5±0.6 Ma (Trung et al., 2007); SHRIMP U-Pb zircon method yields ages of 30.8-26.9 Ma (Bui, 2008); zircon LA-ICP-MS U-Pb ages of 28.62-24.70 Ma (Trinh et al., 2021); zircon LA-ICP-MS U-Pb ages of 26.65±0.33-23.89±0.15 Ma (Bui et al., 2022). Additionally, ⁴⁰Ar/³⁹Ar isotope analysis results for biotite found in granite rocks pegmatite with an age of 25.5±0.5 Ma (Garnier et al., 2002) (Fig. 1b).

2.2. Characteristic ore deposit geology

Tanky is located in the southeast of the Phuhoat uplifted structure (Fig. 1b and Fig. 2) (Le et al., 1994; Tri, 2009). Faults develop prominently in this area, particularly the Muonglam-Quyhop fault, Nghiadan fault, Tanky fault. Additionally, there are northeast-southwest trending faults and sub-meridional faults (Fig. 2). Among these, the Nghiadan and Tanky fault systems play a key role in controlling the geological structure and mineralization in the area in the northeast-southwest direction.

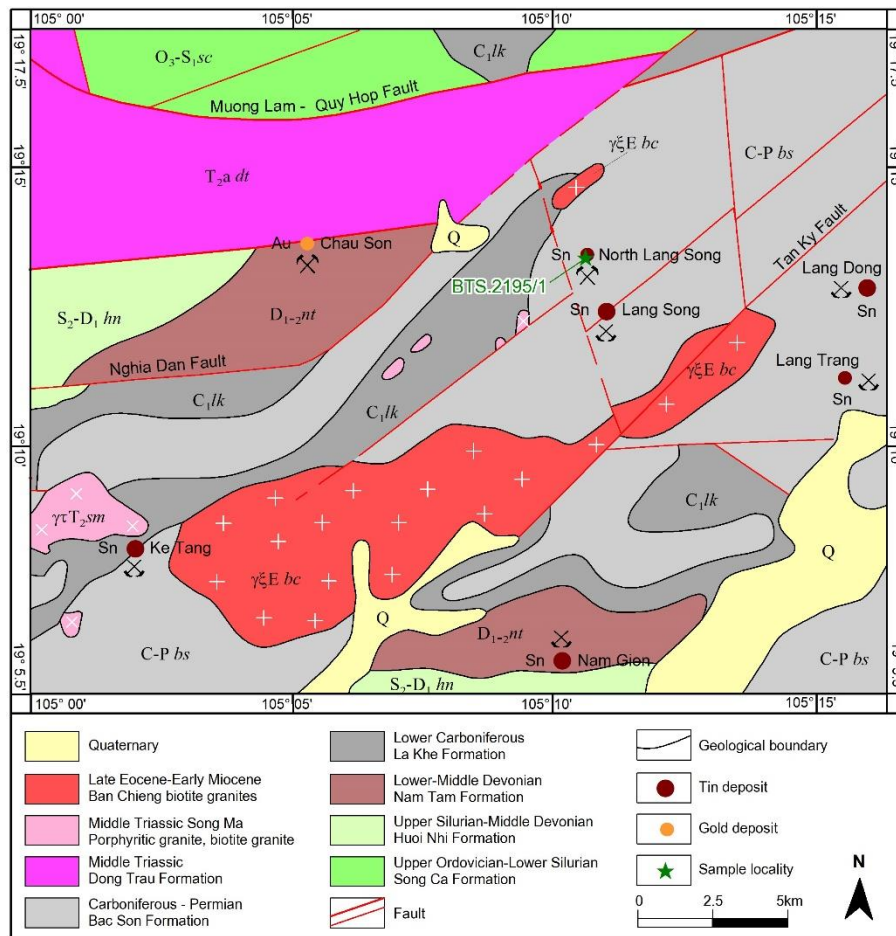


Fig. 2. Geological map of the Tanky area (Le et al., 1994)

Tanky-Quyhop is the area with the largest tin ore reserves in Vietnam. Tin ore was first discovered in the 1965 by Dovjikov et al. (1965). Later, many research, evaluation, and exploration projects uncovered additional tin ore occurrences, often of greisen, skarn, and hydrothermal quartz origin. The tin ore sample used in this study were taken from hydrothermal quartz veins distributed in marble at the North Langsong tin mine (Fig. 2).

Sediments and metamorphic rocks exposed in the Tanky area include: (1) The Upper Ordovician-Lower Silurian Songca formation, comprising sericite schist, quartz-sericite schist, quartz-sericite-graphite schist, and clay shale; (2) the Upper Silurian-Middle Devonian Huoinhi formation, comprising sericitic shale, sandstone and siltstone; (3) the Lower-Middle Devonian Namtam formation, comprising shale, siltstone and sandstone; (4) the Lower Carboniferous Lakhe formation, comprising conglomerate, sandstone, siltstone, siliceous shale and thin-bedded limestone; (5) the Carboniferous-Permian Bacson formation, comprising limestone, marbleized limestone and marble; and (6) the Middle Triassic Dongtrau formation, comprising clastic sediment, tuff sandstone, tuff siltstone and rhyolite (Fig. 2) (Le et al., 1994).

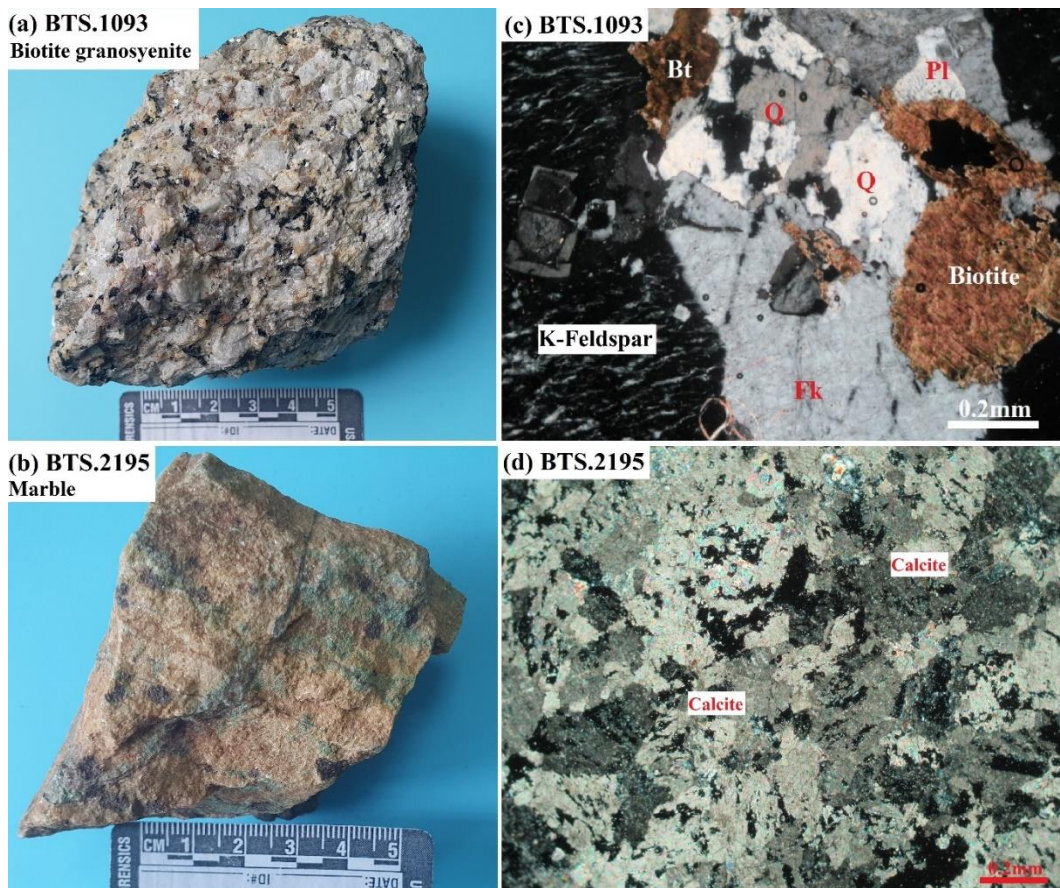


Fig. 3. (a,b) Rock sample photographs and (c,d) petrographic thin sections under optical polarizing microscope, Nikon (+) of biotite granosyenite and tin-ore bearing marble at the North Langsong tin deposits. (a,c) Coarse-grained biotite granosyenite; (b, d) Marbleized limestone, marble. Plagioclase (Pl), quartz (Q), biotit (Bt) and K-feldspar (Fk)

The intrusion rocks of the Banchieng complex are exposed in the center of the study area, forming a large block with an area of about 65 km², a width of 2-5 km, and extending more than 20 km in the northeast-southwest direction. They cut through carbonate, terrigenous sedimentary rocks interbedded with carbonate rocks of the Bacson and Lakhe formations (Fig. 2) (Le et al., 1994).

Biotite granite and biotite granosyenite have massive structures and a large-grained phenocryst texture, with many grains larger than 1 cm in size. They exhibit opalescent colors ranging from gray-white to patchy, with many black cylindrical grains, and are tightly bound with agglutination (Fig. 3a). The lithological composition mainly includes potassium feldspar (55-57%), plagioclase (20-23%), quartz (12-13%), biotite (7-8%), hornblende (2-3%), and some secondary minerals such as apatite, zircon, and sphene. Potassium feldspar exhibits both plate-like and grain-like forms, with subhedral granules to polymorphic textures, and a grain size greater than 1 cm. Plagioclase occurs in plate form, exhibiting sheet, cylindrical, and self-shaped characteristics, with sizes of 2x4.5 mm and multi-twin crystals. Quartz consists of small, polymorphic, colorless, and transparent grains that fill the spaces between feldspar minerals. Biotite displays plate-like to flaky forms, is panidiomorphic, and exhibits multicolored variations from dark brown to light yellow with colorful interference, showing no alteration (Fig. 3c). Hornblende is rare, exhibiting plate-like and cylindrical forms, is dark green, strongly fractured, and interspersed with biotite. Secondary minerals are rare, appearing as small rectangular grains of sphene; less common are small cylindrical grains of apatite and zircon.

The tin mineralization process in Tanky mainly occurs in thick layers of limestone, and marble stone of the Bacson floor system, fault systems (Fig 2 and Fig 3b, d). The lithological composition mainly includes calcite (95-98%), iron hydroxide (1-2%), clay mineral (1-3%). Some mineralization points were discovered in siltstone, shale, shale limestone, and thinly divided limestone of the Lakhe formation and Namtam formations. The mineralization process is closely associated with the fault system of Tanky, which develops in a northeast-southwest direction.

The North Langsong tin deposits are located in the southeast of the Phuhoat uplifted structure. (Fig. 1b and Fig. 2). It belongs to Tanhop commune, Tanky district, and Nghean province. Mineralization

develops in a broken rock zone, 30-50 m wide and extending about 1 km in the northeast-southwest direction, with a dip direction azimuth to the southeast, angle of dip from 30 to 50°. Broken rock zone cuts through limestone layers, marmorized limestone, and marble Bacson formation. The ore bodies often coincide with the broken rock zone. Along the ore zones in the broken rock zone, there are mainly alterations of the surrounding rocks, such as quartzization, sericitization, chloritization, and less commonly, tourmalinization. The ore bodies are usually vein or lenticular and have a northeast-southwest orientation, azimuth of dip direction to the southwest, and dip angle from 30 to 50°. Their lengths usually range from 50 to 100 m or up to 150 m, thickness varies from 0.5-3 m (Fig. 4a).

Ore mineral composition is complex. The common primary mineral ores include pyrite (15-40%), cassiterite (1-5%), arsenopyrite, chalcopyrite (1-2), galena (3-4%), and bismuth (1%), less common are ilmenite, pyrrhotite, hematite, manganite. Secondary mineral ores include limonite, scorodite, cerussite, psilomelane. Gangue-free minerals include quartz with tourmaline (10-15%), sericite, chlorite (4-5%), muscovite, biotite (3-4%), kaolinite (Fig. 4). The process of ore formation includes two stages: (1) the first stage forms a quartz-tourmaline complex containing cassiterite and minerals containing iron, magnesium, manganese. This is the main complex of hydrothermal veins, the tourmaline content usually decreases from the inside to the outside of the vein (Fig. 4b,d) and (2) later stage forms pyrite, cassiterite, bismuth association. **Minerals** have a stacked or cross-sectional structure of minerals of the early stage. (Fig. 4c,e,f).

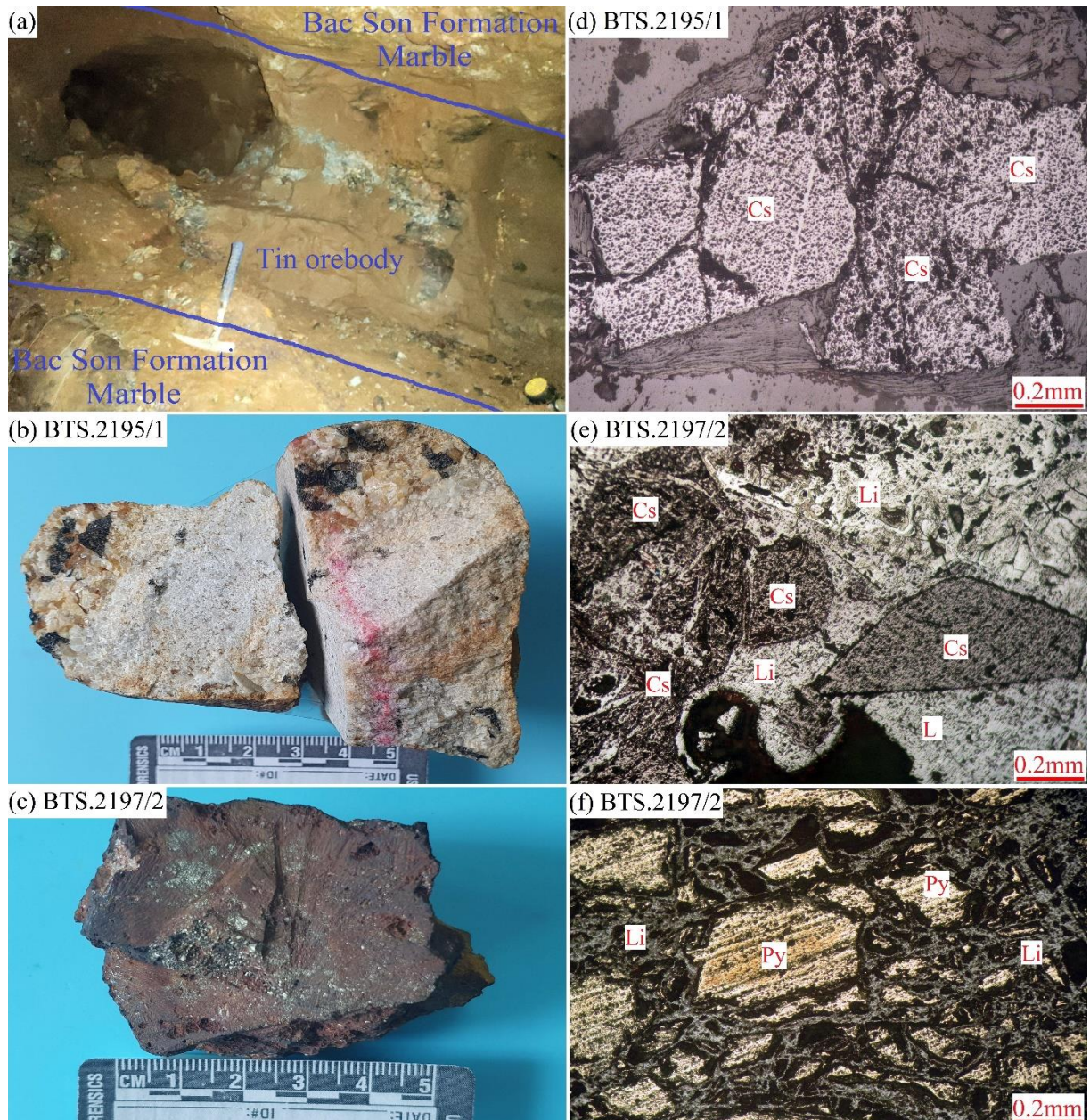


Fig. 4. (a,b,c) Photographs and (d,e,f) polished sections of rock samples from the North Langsong tin deposits: (a) tin ore body at mine tunnel; (b) cassiterite associated with tourmaline-bearing quartz; (c)

cassiterite associated with limited pyrite; (d) cassiterite nest in non-ore quartz matrix; (e) cassiterite associated with sulfur mineral completely limonized, pseudomorph substitution; (f) partially limonized pyrite. Cassiterite (Cs), Pyrite (Py), Limonite (Li).

3. Analytical methods

Monomeric cassiterite used to determine the age of the ore was taken from the mine tunnel at the North Langsong mine, Tanky, Nghean. Cassiterite specimens were dated using the LA-ICP-MS U-Pb isotopic method. Sample BTS.2195/1 was obtained from a hydrothermal tin-quartz ore body in a marble of the Bacson formation (Fig. 1b; Fig. 2 and Fig. 4a). The sampling location has geographical coordinates of 19° 13' 22" N and 105° 10' 35" E. Cassiterite grains are typically brown to dark brown (Fig. 5b).

The ore sample was taken from the mine, then crushed and sieved through a sieve with a mesh size of 0.5-1 mm. The sample was then sieved and washed, with heavy minerals separated using a bromoform heavy solution, then dried and magnetic minerals are separated. The cassiterite grains were selected under a stereomicroscope and examined under a binocular microscope. The grains were carefully inspected for surface alterations, impurities, and cracks. Using a standard sample (AY-4) with an isotope dilution-thermal ionization mass spectrometry measurement, yielding a U-Pb isotopic age of 158.2 ± 0.4 Ma for comparison (Yuan et al., 2011). The internal structure of cassiterite was analyzed using scanning electron microscopy (SEM) and cathodoluminescence (CL) imaging.

Each set of six spot analyses was followed by three analyses of AY-4 (Yuan et al., 2011) and one analysis of NIST SRM 612 (Kent, 2008; Jenner et al., 2009). The laser produced an ablation pit with a diameter of 50 μm at a pulse rate of 8 Hz and energy density of 4 J/cm^2 in the analysis of these cassiterite grains. Each analysis consisted of approximately 20 s of background acquisition, followed by 40 s of data acquisition, with a 50 s delay between analyses. During the U-Pb dating process, the dwell time of each mass scan was set to 25 ms for ^{238}U , ^{232}Th , ^{208}Pb , ^{206}Pb , ^{204}Pb , and ^{202}Hg and 40 ms for ^{207}Pb .

Determining the U-Pb cassiterite isotopic age was performed using equipment Agilent 7900 ICP-MS instrument in combination with a RESOLUTION S-155 193 nm excimer ArF laser ablation system (Australian Scientific Instruments Pty Ltd, Australia) at the Tianjin Center of China Geological Survey, Tianjin 300170, China. Raw data reduction was performed offline using the ICPMSDataCal 10.9 software. The uncorrected cassiterite composition measurements were plotted on a Tera-Wasserburg Concordia diagram. The cassiterite U-Pb age calculation and Concordia diagrams were generated online using the software IsoplotR. Uncertainty was determined at the 2σ .

Tab. 1. LA-ICP-MS U-Pb dating results for cassiterite samples from the North Langsong deposit.

Sample spots BTS.2195/1	Isotopic ratios and errors ($\pm 1\sigma$)						Ages (Ma) and errors ($\pm 1\sigma$)			
	$^{207}\text{Pb}/^{206}\text{Pb}$	1σ	$^{207}\text{Pb}/^{235}\text{U}$	1σ	$^{206}\text{Pb}/^{238}\text{U}$	1σ	$^{207}\text{Pb}/^{235}\text{U}$	1σ	$^{206}\text{Pb}/^{238}\text{U}$	1σ
1	1,0429	0,3563	5,6620	0,6349	0,0607	0,0062	1926	97	380	37
2	0,2902	0,0778	0,2526	0,0335	0,0080	0,0004	229	27	51	3
3	0,8624	0,1773	1,3915	0,1174	0,0160	0,0012	885	50	103	8
4	0,7895	0,1084	10,9138	1,1310	0,1285	0,0159	2516	96	779	91
5	1,2947	0,3493	1,8199	0,2909	0,0192	0,0036	1053	105	122	23
6	0,7600	0,0849	2,1830	0,1473	0,0254	0,0013	1176	47	162	8
7	0,4015	0,2148	2,8128	0,7148	0,0332	0,0077	1359	190	211	48
8	0,0652	0,1655	0,3496	0,0882	0,0094	0,0010	304	66	60	6
9	0,0000	0,0000	0,2383	0,0816	0,0094	0,0014	217	67	60	9
10	0,5839	0,0459	10,1089	0,5228	0,1287	0,0057	2445	48	781	33
11	0,0000	0,0000	1,1316	0,1862	0,0183	0,0025	769	89	117	16
12	0,0000	0,0000	1,5526	0,1329	0,0230	0,0022	952	53	147	14
13	0,5660	0,0294	28,0559	1,2215	0,3626	0,0190	3421	43	1994	90
14	0,0000	0,0000	0,3130	0,1581	0,0067	0,0026	277	122	43	16
15	0,5328	0,0229	11,7644	1,2278	0,1604	0,0164	2586	98	959	91
16	0,1152	0,0713	0,0481	0,0317	0,0061	0,0006	48	31	39	4
17	0,1507	0,1706	0,3602	0,1863	0,0091	0,0020	312	139	58	13
18	0,2688	0,1657	0,3881	0,1750	0,0078	0,0028	333	128	50	18
19	0,2113	0,4072	0,1456	0,0838	0,0066	0,0012	138	74	43	8
20	0,0000	0,0000	0,9950	0,2713	0,0199	0,0027	701	138	127	17
21	0,0000	0,0000	0,0469	0,0543	0,0060	0,0008	47	53	39	5
22	0,0469	0,1198	0,0513	0,0348	0,0049	0,0006	51	34	32	4
23	0,0166	0,1373	0,7876	0,6146	0,0108	0,0072	590	349	69	46
24	0,0000	0,0000	0,9263	0,2534	0,0224	0,0040	666	134	143	25
25	0,1163	0,1331	0,1742	0,0999	0,0063	0,0010	163	86	40	7

4. Results

The cassiterite grains obtained from the sample selected for analysis were yellow-brown to dark brown and had small cracks (Fig. 5). Cathodoluminescence imaging shows that most cassiterite grains are monohedral or subhedral in shape, 100 to 450 μm long, and 80 to 300 μm wide. The largest cassiterite grains, averaging 300 μm in length and 250 μm in width. Shapes range from granular to polymorphic and short prismatic. Some cassiterite grains exhibit strong cathodoluminescence.

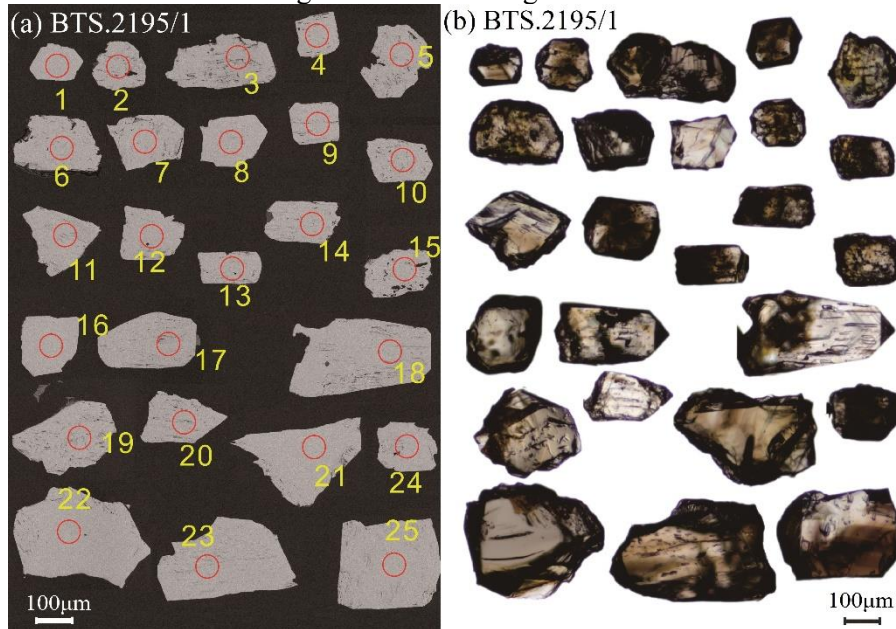


Fig. 5. (a) Cathodoluminescence (CL) and (b) Optical polarizing microscope images of cassiterite grains from the North Langsong tin deposits. The red circle is the location of the U-Pb zircon isotope analysis spots.

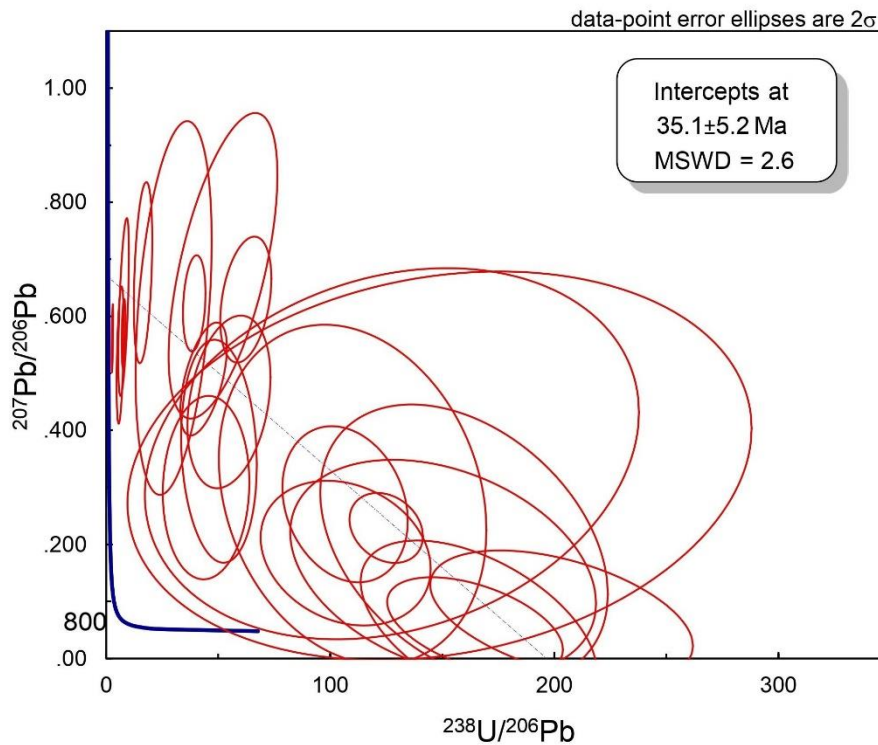


Fig. 6. Tera-Wasserburg Concordia $^{238}\text{U}/^{206}\text{Pb}$ - $^{207}\text{Pb}/^{206}\text{Pb}$ diagram of cassiterite from the North Langsong tin deposits.

The analytical points used in the LA-ICP-MS U-Pb determination method were chosen carefully to avoid locations with cracks and impurities. The analytical results for sample BTS.2195/1 are shown in Table 1 and the Tera-Wasserburg Concordia diagram illustrates the intersection curve of the isotopic ratios of $^{207}\text{Pb}/^{206}\text{Pb}$ versus $^{238}\text{U}/^{206}\text{Pb}$ in Figure 6. 25 spots on cassiterite mineral from sample BTS.2195/1 were analysed (Fig. 5a). The ratios of $^{238}\text{U}/^{206}\text{Pb}$ and $^{207}\text{Pb}/^{206}\text{Pb}$ were 0.0-1.2947 and 0.0049-0.3626 (Table 1). The analytical results for the high confidence intersection age are 35.1 ± 5.2 Ma (MSWD = 2.6, 2σ) (Fig. 6). Thus, based on the age intersection obtained from the hydrothermal cassiterite of the North Langsong mine, it can be affirmed that the tin ore in the Tanky Nghean area has a formation age of about 35.1 ± 5.2 Ma corresponding to the Late Eocene - Early Oligocene.

5. Discussion

5.1. Age position of the Banchieng complex

Previous studies have shown that the granitoid magmatic rocks of the Banchieng complex in the Phuhoat uplifted structure in the North Central region of Vietnam are of the Late Paleogene age (Table 2; Fig. 1b; Fig. 7) (Lepvrier et al., 1997; Jolivet et al., 1999; Nagy et al., 2000; Garnier et al., 2002; Trung et al., 2007; Nguyen et al., 2014; Bui et al., 2017; Trinh et al., 2021). Biotite $^{40}\text{Ar}/^{39}\text{Ar}$ isotopic analysis results also show the age ranging from 27.3 to 22.1 Ma for biotite granite and pegmatite (Lepvrier et al., 1997; Jolivet et al., 1999; Garnier et al., 2002). Trung et al., 2007, when studying the alkaline feldspar porphyry granites of the Banchieng complex in Quephong area, the Rb-Sr isotope gave the age on the whole-rock is 27 ± 1 Ma and the K-Ar biotite age is 24.7-24.2 Ma. Bui (2008), when analyzing zircon TIMS U-Pb isotopes of granosyenite rocks in Quyhop area gave the age of 30.8 ± 2 Ma.

In recent years, many authors have attempted to determine the age of granitoid rocks of the Banchieng complex using modern and highly accurate analytical methods. Results of zircon U-Pb isotope analysis using the SHRIMP method gave the age of 27.36 ± 0.36 - 27.47 ± 0.5 Ma (Nguyen et al., 2014), and 27.5 ± 0.6 - 29.5 ± 0.4 Ma (Bui et al., 2017). Trinh et al., 2021 and Bui et al., 2022 analyzed U-Pb zircon isotopic ages using the laser ablation inductively coupled plasma mass spectrometry (LA-ICP-MS) for ages ranging from 23.89 ± 0.15 to 28.62 ± 0.89 Ma.

Thus, the granitoid rocks of the Banchieng Complex cover a relatively wide age range from 30.8 to 22.1 Ma, corresponding to the Oligocene-Early Miocene.

Tab. 2. Summary of formation ages of granitoid rocks from the Banchieng Complex and tin ores Quyhop-Tanky area.

No.	Sample name	Rock type	Mineral analyzed	Dating method	Result (Ma)	References
1	VN230	Pegmatite	Biotite	Ar-Ar	22.1 ± 1.3	(Lepvrier et al., 1997)
2	VN9717	Granite	Biotite	Ar-Ar	27.3 ± 0.5	(Jolivet et al., 1999)
3	VN9705	Granite	Biotite	Ar-Ar	26.4 ± 1.1	(Jolivet et al., 1999)
4	VGS-32	Granite	Monazite	U-Pb	26.0 ± 0.2	(Nagy et al., 2000)
5	VGS-33	Granite	Monazite	U-Pb	23.7 ± 1.6	(Nagy et al., 2000)
6	MC-12	Pegmatite	Biotite	Ar-Ar	22.5 ± 0.5	(Garnier et al., 2002)
7	FL13	Granite	Biotite	K-Ar	24.5 ± 0.6	(Trung et al., 2007)
8	BCG	Porphyritic granite	Biotite	Rb-Sr	27 ± 1	(Trung et al., 2007)
9		Granosyenit	Zircon	TIMS U-Pb	$30,8 \pm 2$	(Bui., 2008)
10	BK-105	Biotite granite	Zircon	SHRIMP U-Pb	27.36 ± 0.36	(Nguyen et al., 2014)
11	TL156	Biotite granite	Zircon	SHRIMP U-Pb	27.47 ± 0.5	(Nguyen et al., 2014)
12	TL-137	Granosyenite	Zircon	SHRIMP U-Pb	29.5 ± 0.4	(Bui et al., 2017)
13	TL-234	Porphyritic granite	Zircon	SHRIMP U-Pb	27.2	(Bui et al., 2017)
14	TL-135	Porphyritic granite	Zircon	SHRIMP U-Pb	27.5 ± 0.6	(Bui et al., 2017)
15	L-019	Porphyritic granite	Zircon	LA-ICP-MS U-Pb	24.70 ± 0.18	(Trinh et al., 2021)
16	L-030	Porphyritic granite	Zircon	LA-ICP-MS U-Pb	28.35 ± 0.28	(Trinh et al., 2021)
17	H-VN-012	Alskite granite	Zircon	LA-ICP-MS U-Pb	28.62 ± 0.89	(Trinh et al., 2021)
18	H-VN-002	Granosyenite	Zircon	LA-ICP-MS U-Pb	28.17 ± 0.52	(Trinh et al., 2021)

19	BN-BC3	Biotite granite	Zircon	LA-ICP-MS U-Pb	26.65 ± 0.33	(Bui et al., 2022)
20	CT-BC	Biotite granite	Zircon	LA-ICP-MS U-Pb	23.89 ± 0.15	(Bui et al., 2022)
21	SB-1	Quartz tin ore	Cassiterite	LA-ICP-MS U-Pb	26.81 ± 1.92	(Bui et al., 2022)
22	BN-Gre	Greisen tin ore	Cassiterite	LA-ICP-MS U-Pb	23.23 ± 0.89	(Bui et al., 2022)
23	BN-Gre	Greisen tin ore	Muscovite	Ar-Ar	23.85 ± 0.16	(Bui et al., 2022)
24	BTS.2195/1	Tin-quartz ore	Cassiterite	LA-ICP-MS U-Pb	35.1±5.2	(this study)

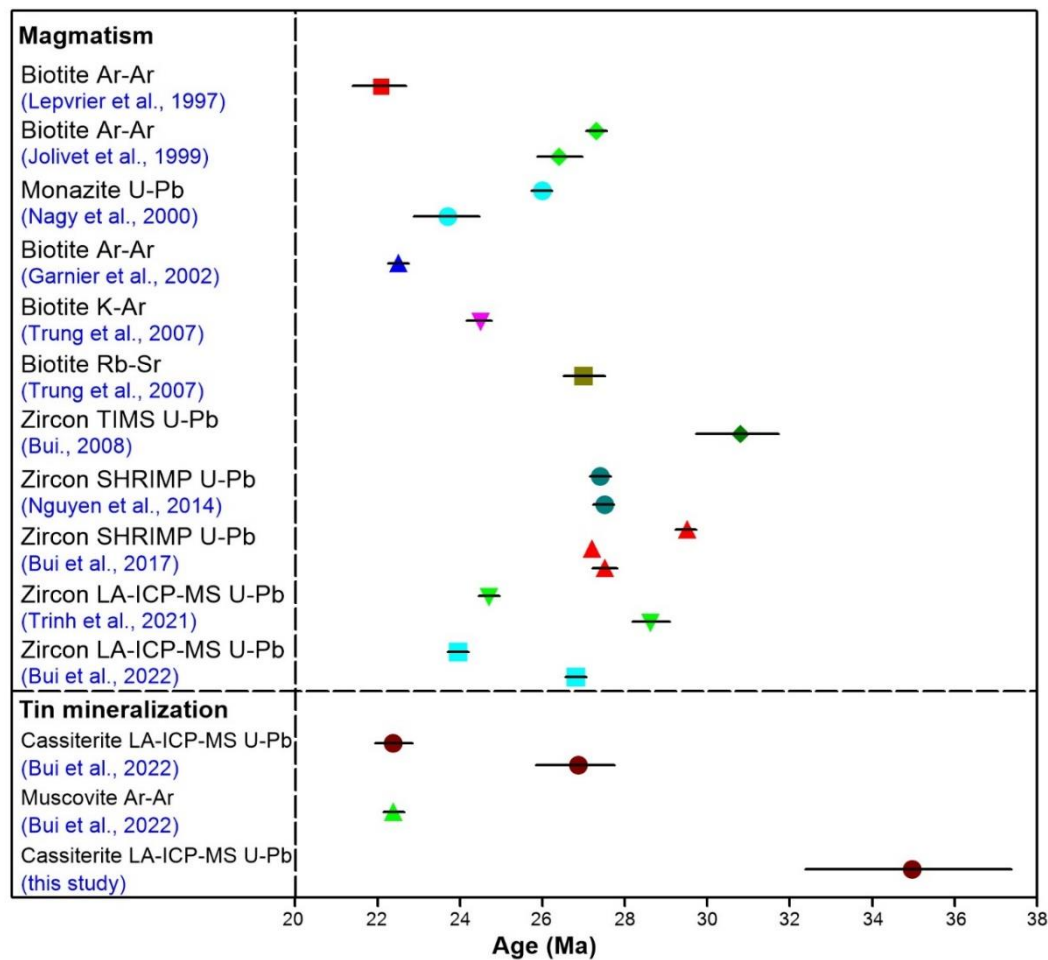


Fig. 7. Age chart of the Banchieng complex and tin ores Quyhop-Tanky in the Phuhoat uplifted structure (data from Table 2).

5.2. Age of tin mineralisation at Tanky

In some parts of the world, the age determination of tin ore deposits from cassiterite U-Pb dating with the use of the laser ablation inductively coupled plasma mass spectrometry (LA-ICP-MS) has been successfully performed (Chen et al., 2014; Cao et al., 2017; Zhang et al., 2019a, 2020; Moscati and Neymark, 2020, Bui et al., 2022). In the North Central, Vietnam only has the study of Bui et al (2022) studying the age of tin ore using the Cassiterite LA-ICP-MS U-Pb method for Suoibac and Banngoc deposit.

LA-ICP-MS U-Pb results on cassiterite grains from sample BTS.2195/1 indicate an age of 35.1 ± 5.2 Ma (Fig. 6). This result shows that the age of tin deposit formation in the Tanky area is older than that of tin deposit formation in the Quyhop area (Duong et al., 1983; Bui et al., 2022). According to Bui et al. (2022), the age of muscovite ⁴⁰Ar/³⁹Ar from greisen ore in the Banngoc mine (Quyhop) is 23.85 ± 0.16 Ma and the age of U-Pb cassiterite from quartz ore in the Suoibac mine (Quyhop) is 23.23 ± 0.89 Ma. The U-P age analysis of cassiterite from North Langsong tin ore is 35.1 ± 5.2 Ma. Thus, tin mineralization in the Tanky area was formed in the Late Eocene period and tin mineralization at the Phuhoat uplifted structure can last from the Late Eocene.

5.3. Origin relationship between Banchieng granite and tin mineralization in the Phuhoat uplifted structure

Most endogenous ore deposits and tin deposits are closely associated with the intrusion of granite, especially biotite granites (Hosking, 1977; Taylor, 1979; Hutchison, 1984; Olade, 1980; Zhang et al., 2015; Zhang et al., 2017b). According to Duong et al. (1983) and Bui et al. (2022), the Banchieng Complex granite is closely related to the tin mineralization in the Quyhop-Tanky.

The results of age determination show that the granitoid of Banchieng complex was formed from 30.8 to 22.1 Ma (Table 2). Muscovite $^{40}\text{Ar}/^{39}\text{Ar}$ and LA-ICP-MS cassiterite U-Pb analysis results indicate that the tin deposits in Tanky-Quyhop have an era of 31.5 ± 5 -23.23 Ma (Table 2; Fig. 7). A comparison of magmatic activity time and ore formation period in the study area shows that the appearance of biotite granite may have led to the formation of tin mineralization in the Late Eocene-Oligocene. Thus, the Paleogene granitoid of the the Banchieng complex in the Phuhoat uplifted structure raised has a close relationship in space and time with the tin body ores in the area.

6. Conclusion

The North Langsong tin deposits are located in the Tanhop commune, Tanky district, Nghean, and have a hydrothermal genesis associated with quartz and sulfur mineralization. The ore bodies are in the broken rock zone with a northeast - southwest orientation, striking southeast, and dipping from 30° to 50° . Mineralization zone developed in thick-bedded limestone, marble, from the Carboniferous-Permian age of the Bacson formation.

The results of cassiterite U-Pb isotopic age determination using LA-ICP-MS U Pb method show that the age of quartz-sulfur tin ore in the North Langsong deposit is 35.1 ± 5.2 Ma. Tin mineralization of the Tanky has been formed in the Late Eocene-Oligocene having a close spatial and temporal relationship with the Paleogene biotite granite, biotite granosyenite of the Banchieng complex in the Phuhoat uplifted structure. However, the research only focused on the central area of the Phuhoat uplifted structure, and further studies are needed to confirm the origin of tin mineralization in the whole Tanky area.

Acknowledgements

The authors thank Vietnam's Ministry of Natural Resources and Environment for the grant to implement the topic "Magma evolution research-tectonics of Permi-Triassic age granitoid formations North of the Truongson belt and endogenous mineral potential". Code: TMNT.2022.562.02. We also like to thank the anonymous reviewers for their valuable remarks that greatly contribute to the quality of the paper.

Declaration of Competing Interest

The authors declare that they have no competing interests.

Literature - References

1. Bai, X.J., Wang, M., Jiang, Y.D., Qiu, H.N., 2013. Direct dating of tin-tungsten mineralization of the Piaotang tungsten deposit, South China, by $^{40}\text{Ar}/^{39}\text{Ar}$ progressive crushing. *Geochim. Cosmochim. Acta* 114, 1-12.
2. Bui, D.C., Qiu, H.N., Ngo, X.D., Bai, X.J., W, Y., 2022. Dating of granite-related tin mineralisation at Quyhop, Vietnam: Constraints from zircon and cassiterite U-Pb and muscovite $^{40}\text{Ar}/^{39}\text{Ar}$ geochronology. *Ore Geology Reviews* 143 (2022) 104785, 1-16.
3. Bui, D.C., Nguyen, T.B.T., Nguyen, C.D., Ta, D.T., 2017. SHRIMP zircon U-Pb isotope age of Banchieng granitoid in Phuhoat structural zone and its geological implication. *Journal of GEOLOGY, Series B*, No.46/2017, p. 14-22.
4. Bui, M.T., 2008. Completing the Vietnamese magma scale from a global tectonic perspective. *Geological Archives Center, Hanoi*.
5. Cao, H.W., Zhang, Y.H., Pei, Q.M., Zhang, R.Q., Tang, L.i., Lin, B., Cai, G.J., 2017. U-Pb dating of zircon and cassiterite from the Early Cretaceous Jiaojiguan iron-tin polymetallic deposit, implications for magmatism and metallogeny of the Tengchong area, western Yunnan. *China. Int. Geol. Rev* 59 (2), 234-258.

6. Carter, A., Roques, D., Bristow, C., Kinny, P., 2001. Understanding Mesozoic accretion in Southeast Asia: significance of Triassic thermotectonism (Indosinian orogeny) in Vietnam. *Geology* 29 (3), 211.
7. Chen, X.C., Hu, R.Z., Bi, X.W., Li, H.M., Lan, J.B., Zhao, C.H., Zhu, J.J., 2014. Cassiterite LA-MC-ICP-MS U/Pb and muscovite $40\text{Ar}/39\text{Ar}$ dating of tin deposits in the Tengchong-Lianghe tin district, NW Yunnan, China. *Mineral. Deposita* 49 (7), 843-860.
8. Dovjikov, A., Bao, N.X., Van Chien, N., Luong, T.D., Van Quang, P., Izok, E., Marisev, A., Long, P.D., Zamoida, A., Ivanov, G., 1965. *Geology of Northern Vietnam*, Technical and Scientific Publisher, Hanoi (in Vietnamese), pp. 583.
9. Duong, D.K., Shachnovsky, M.L., Le, V.T., Nguyen, V.N., Nguyen, T.K.H., Thai, Q.L., Nguyen, N.L., Do, H.D., Pham, V.L., 1983. Tin metallogeny of Vietnam. *J. Geol. (in Vietnamese)* 162, 12-16.
10. Duong, V.H., Phan, T.T., Nguyen, T.D., Piestrzyski, A., Nguyen, D.C., Pieczonka, J., Ngo, X.D., Tran, V.P., Pham, T.B., Nguyen, V.H., Ngo, V.L., Bui, T.D., Vu, K.D., Bui, C.T., 2021. Cu-Au mineralization of the Sin Quyen deposit in north Vietnam: A product of Cenozoic left-lateral movement along the Red River shear zone. *Ore Geol. Rev.* 132, 104065.
11. Fromaget, J., 1941. L'Indochine Francaise, sa structure geologique, ses roches, ses mines et leur relation possible avec la tectonique. *Bull. Serv. Geol. Indoch.* 26, 140 pp.
12. Garnier, V., Giuliani, G., Maluski, H., Ohnenstetter, D., Phan, T.T., Hoang, Q.V., Pham, V. L., Vu, V.T., Schwarz, D., 2002. Ar-Ar ages in phlogopites from marble-hosted ruby deposits in northern Vietnam: evidence for Cenozoic ruby formation. *Chem. Geol.* 188 (1-2), 33-49.
13. Gulson, B.L., Jones, M.T., 1992. Cassiterite: Potential for direct dating of mineral deposits and a precise age for the Bushveld Complex granites. *Geology* 20 (4), 355. Harrison, T.M., Celerier, J., Aikman, A.B., Hermann, J., Heizler, M.T., 2009. Diffusion of 40Ar in muscovite. *Geochim. Cosmochim. Acta* 73 (4), 1039-1051.
14. Hieu, P. T., Li, S. Q., Yu, Y., Thanh, N. X., Dung, L. T., Tu, V. L., Siebep, W., & Chen, F., 2016. Stages of late Paleozoic to early Mesozoic magmatism in the Songma belt, NW Vietnam: evidence from zircon U–Pb geochronology and Hf isotope composition. *International Journal of Earth Sciences*, Volume 106, Issue3, p. 855-874, <http://doi.org/10.1007/s00531-016-1337-9>.
15. Hosking, K.F.G., 1977. Known relationships between the 'hard-rock' tin deposits and the granites of Southeast Asia. *Bull. Geol. Soc. Malays.* 9, 141-157.
16. Hutchison, C., 1984. *Geology of tin deposits in Asia and the Pacific*, Selected papers from the International Symposium on the Geology of tin deposits, held in Nanning, China, pp. 26-30.
17. Jenner, F.E., Holden, P., Mavrogenes, J.A., O'Neill, H.S., Allen, C., 2009. Determination of selenium concentrations in NIST SRM 610, 612, 614 and geological glass reference materials using the electron probe, LA-ICP-MS and SHRIMP II. *Geostand. Geoanal. Res.* 33 (3), 309-317.
18. Jolivet, L., Maluski, H., Beyssac, O., Goff'e, B., Lepvrier, C., Thi, P.T., Vuong, N.V., 1999. Oligocene-Miocene Bukhang extensional gneiss dome in Vietnam: geodynamic implications. *Geology* 27 (1), 67.
19. Jolivet, L., Beyssac, O., Goff'e, B., Avigad, D., Lepvrier, C., Maluski, H., Thang, T.T., 2001. Oligo-Miocene midcrustal subhorizontal shear zone in Indochina. *Tectonics* 20 (1), 46-57.
20. Kamvong, T., Khin Zaw, Meffre, S., Maas, R., Stein, H., Lai, C.K., 2014. Adakites in the Truongson and Loei fold belts, Thailand and Laos: Genesis and implications for geodynamics and metallogeny. *Gondwana Res.* 26 (1), 165-184.
21. Kent, A.J.R., 2008. Lead isotope homogeneity of NIST SRM 610 and 612 glass reference materials: Constraints from laser ablation multicollector ICP-MS (LA-MC-ICP-MS) analysis. *Geostand. Geoanal. Res.* 32 (2), 129-147.
22. Le, D.B., Nguyen, V.H., Dang, T.Q., 1994. 1:200.000 Geological and Mineral Map of Vinh area. Published and copyright by Geological survey of Vietnam, Hanoi.
23. Le, D.B., Dang, T.Q., Dinh, M.M., Le, D.K., Nguyen, N.M., Nguyen, V.M., Nguyen, T.N., Nguyen, T.C., Nguyen, V.S., Pham, H., Pham, N.C., Tran, P.T., Tran, V.B., 2001. *Geology and Mineral Resources Map of Vietnam Scale 1:200,000, Thanhhoa Sheet (E-48-IV)*. Department of Geology and Minerals of Vietnam, Hanoi (in Vietnamese), p. 126.
24. Lehmann, B., 1982. Metallogeny of tin; magmatic differentiation versus geochemical heritage. *Econ. Geol.*, 77: 50-59.

25. Lepvrier, C., Maluski, H., Nguyen, V.V., Roques, D., Axente, V., Rangin, C., 1997. Indosinian NW-trending shear zones within the Truongson belt (Vietnam) ^{40}Ar - ^{39}Ar Triassic ages and Cretaceous to Cenozoic overprints. *Tectonophysics* 283 (1-4), 105-127.
26. Li, C.Y., Zhang, R.Q., Ding, X., Ling, M.X., Fan, W.M., Sun, W.D., 2016. Dating cassiterite using laser ablation ICP-MS. *Ore Geol. Rev* 72, 313-322.
27. Lin, J., Liu, Y., Yang, Y., Hu, Z., 2016. Calibration and correction of LA-ICP-MS and LA-MC-ICP-MS analyses for element contents and isotopic ratios. *Solid Earth Sci.* 1 (1), 5-27.
28. Liu, Y., Li, Z., Li, H., Guo, L., Xu, W., Ye, L., Li, C., Pi, D., 2007. U-Pb geochronology of cassiterite and zircon from the Dulong Sn-Zn deposit: Evidence for Cretaceous large-scale granitic magmatism and mineralization events in southeastern Yunnan province. *China. Acta Petrol. Sin.* 23 (5), 967-976.
29. Liu, Y., Gao, S., Hu, Z., Gao, C., Zong, K., Wang, D., 2010. Continental and oceanic crust recycling-induced melt-peridotite interactions in the Trans-North China Orogen: U-Pb dating, Hf isotopes and trace elements in zircons from mantle xenoliths. *J. Petrol.* 51 (1-2), 537-571.
30. Liu, J., Tran, M., D., Tang, Y., Nguyen, Q.-L., Tran, T.H., Wu., W., Chen, J., Zhang, Z., Zhao, Z., 2012a. Permo-Triassic granitoids in the northern part of the Truongson belt, NW Vietnam: geochronology, geochemistry and tectonic implications. *Gondwana Res.* 22 (2), 628-644.
31. Machado, N., Simonetti, A., 2001. U-Pb dating and Hf isotopic composition of zircon by laser-ablation-MC-ICP-MS. In: Sylvester, P. (Ed.), *Laser Ablation-ICPMS in the Earth sciences: Principles and applications*. Mineralogical Association of Canada, St. John's, Newfoundland, pp. 121-146.
32. Mao, W., Zhong, H., Yang, J.H., Tang, Y.W., Liu, L., Fu, Y.Z., Zhang, X.C., Sein, K., Aung, S.M., Li, J., 2020. Combined zircon, molybdenite, and cassiterite geochronology and cassiterite geochemistry of the Kuntabin tin-tungsten deposit in Myanmar. *Econ. Geol.*, 115: 603-625.
33. Moscati, R.J., Neymark, L.A., 2020. U-Pb geochronology of tin deposits associated with the Cornubian Batholith of southwest England: Direct dating of cassiterite by in situ LA-ICPMS. *Miner. Depos.* 55 (1), 1-20.
34. Nagy, E.A., Schärer, U., Nguyen, T.M., 2000. Oligo-Miocene granitic magmatism in central Vietnam and implications for continental deformation in Indochina. *Terra Nova* 12 (2), 67-76.
35. Neymark, L.A., Holm-Denoma, C.S., Moscati, R.J., 2018. In situ LA-ICPMS U-Pb dating of cassiterite without a known-age matrix-matched reference material: Examples from worldwide tin deposits spanning the Proterozoic to the Tertiary. *Chem. Geol.* 483, 410-425.
36. Nguyen, T.A., Yang, X., Vu, T.H., Liu, L., Lee, I., 2019. Piaoac Granites Related W-Sn Mineralization, Northern Vietnam: Evidences from Geochemistry, Zircon Geochronology and Hf Isotopes. *J. Earth Sci.* 30 (1), 52-69.
37. Nguyen, C.D., Duong, H.S., Nguyen, T.C., Bui, D.C., Nguyen, T.H.T., 2014. Studying Metallogeny and Prospective Division of Mineral Resources in the Phuhoat Structural Zone. *Geological archives, Hanoi (in Vietnamese)*, p. 145.
38. Nguyen, C.D., Duong, H.S., Bui, D.C., Bui, M.T., 2015. U-Pb zircon SHRIMP isotopic age of Namgiai granitoid in Phuhoat (Nghean) and their geodynamic significance, 50th Anniversary of Vietnam Institute of Geosciences and Mineral Resources, Vietnam Institute of Geosciences and Mineral Resources (in Vietnamese with English abstract), pp. 34-39.
39. Olade, M.A., 1980. Geochemical characteristics of tin-bearing and tin-barren granites, northern Nigeria. *Econ. Geol.*, 75: 71-82.
40. Roger, F., Maluski, H., Lepvrier, C., Vu, V.T., Paquette, J.L., 2012. LA-ICPMS zircons U-Pb dating of Permo-Triassic and Cretaceous magmatism in Northern Vietnam-Geodynamical implications. *J. Asian Earth Sci.* 48, 72-82.
41. Schärer, U., Tapponnier, P., Lacassin, R., Leloup, P.H., Zhong, D.L., Ji, S.C., 1990. Intraplate tectonics in Asia: a precise age for large-scale Miocene movement along the Ailao Shan-Red River shear zone. *China. Earth Planet. Sci. Lett.* 97, 65-77.
42. Schärer, U., Zhang, Lian-Sheng, Tapponnier, P., 1994. Duration of strike-slip movements in large shear zones: the Red River belt, China. *Earth Planet. Sci. Lett.* 126 (4), 379-397.
43. Shi, M.F., Lin, F.C., Fan, W.Y., Deng, Q.i., Cong, F., Tran, M.D., Zhu, H.P., Wang, H., 2015. Zircon U-Pb ages and geochemistry of granitoids in the Truongson terrane, Vietnam: Tectonic and metallogenic implications. *J. Asian Earth Sci.* 101, 101-120.

44. Tang, Y., Liu, J., Tran, M.D., Song, Z., Wu, W., Zhang, Z., Zhao, Z., Chen, W., 2013. Timing of left-lateral shearing along the Ailao Shan-Red River shear zone: constraints from zircon U-Pb ages from granitic rocks in the shear zone along the Ailao Shan Range, Western Yunnan, China. *Int. J. Earth. Sci.* 102 (3), 605-626.
45. Taylor, R.G., 1979. *Geology of tin deposits*. Elsevier Scientific Publishing Co, Amsterdam, Netherlands, pp. 1-543 vol. 11.
46. Tran, T.H., Tran, T.A., Ngo, T.P., Pham, T.D., Tran, V.A., Izokh, A.E., Borisenko, A.S., Lan, C.Y., Chung, S.L., Lo, C.H., 2008. Permo-Triassic intermediate-felsic magmatism of the Truongson belt, eastern margin of Indochina. *C. R. Geoscience* 340 (2-3), 112-126.
47. Tran, T.V., Faure, M., Nguyen, V.V., Bui, H.H., Fyhn, M.B.W., Nguyen, T.Q., Lepvrier, C., Thomsen, T.B., Tani, K., Charusiri, P., 2020. Neoproterozoic to Early Triassic tectono-stratigraphic evolution of Indochina and adjacent areas: A review with new data. *J. Asian Earth Sci.* 191, 104231.
48. Tran, V.T., 2009. *Geology and resources of Vietnam*. Science and technology publishing house. Hanoi, 589 p.
49. Tran, V.T., Dao, T.B., Nguyen, X.B., & Nguyen, V.H., 2016. *Geology, Geological resources of Vietnam and the adjacent seas*. Geological Archives Information Center. Hanoi, 240 p.
50. Trinh, D.H., Luu, C.T., Nguyen, T.A., Tran, V.A., Phan, H.G., Nagi, T., Boua, L.S., 2021. Paleogene granite magmatism in the north of the Truongson belt and implication for crustal evolution. *Vietnam J. Earth Sci.* 43, 478-497.
51. Trung, N.M., Nuong, N.D., Itaya, T., 2007. Rb-Sr isochron and K-Ar ages of igneous rocks from the Samnua Depression Zone in Northern Vietnam. *J. Mineral. Petrol. Sci.* 102 (2), 86-92.
52. Wang, X., Yao, X., Wang, S., Zhu, X., Wang, J., Wang, C., 2019. Intraplate extension of the Indochina plate deduced from 26 to 24 Ma A-type granites and tectonic implications. *Int. Geol. Rev.* 61 (14), 1691-1705.
53. Yuan, S., Peng, J., Hu, R., Li, H., Shen, N., Zhang, D., 2008. A precise U-Pb age on cassiterite from the Xianghualing tin-polymetallic deposit (Hunan, South China). *Miner. Depos.* 43 (4), 375-382.
54. Yuan, S., Peng, J., Hao, S., Li, H., Geng, J., Zhang, D., 2011. In situ LA-MC-ICP-MS and ID-TIMS U-Pb geochronology of cassiterite in the giant Furong tin deposit, Hunan Province, South China: New constraints on the timing of tin-polymetallic mineralization. *Ore Geol. Rev.* 43 (1), 235-242.
55. Zaw, K., Meffre, S., Lai, C.K., Burrett, C., Santosh, M., Graham, I., Manaka, T., Salam, A., Kamvong, T., Cromie, P., 2014. Tectonics and metallogeny of mainland Southeast Asia-A review and contribution. *Gondwana Research* 26 (2014), 5-30.
56. Zhang, L.S., Schaerer, U., 1999. Age and origin of magmatism along the Cenozoic Red River shear belt, China. *Contrib. Mineral. Petrol.* 134 (1), 67-85.
57. Zhang, D., Peng, J., Coulson, I.M., Hou, L., Li, S., 2014. Cassiterite U-Pb and muscovite ^{40}Ar - ^{39}Ar age constraints on the timing of mineralization in the Xuebaoding Sn-W-Be deposit, western China. *Ore Geol. Rev.* 62, 315-322.
58. Zhang, R.Q., Lu, J.J., Wang, R.C., Yang, P., Zhu, J.C., Yao, Y., Gao, J.F., Li, C., Lei, Z.H., Zhang, W.L., Guo, W.M., 2015. Constraints of in situ zircon and cassiterite U-Pb, molybdenite Re-Os and muscovite ^{40}Ar - ^{39}Ar ages on multiple generations of granitic magmatism and related W-Sn mineralization in the Wangxianling area, Nanling Range, South China. *Ore Geol. Rev.* 65, 1021-1042.
59. Zhang, R., Lehmann, B., Seltnann, R., Sun, W., Li, C., 2017a. Cassiterite U-Pb geochronology constrains magmatic-hydrothermal evolution in complex evolved granite systems: The classic Erzgebirge tin province (Saxony and Bohemia). *Geology* 45 (12), 1095-1098.
60. Zhang, R., Lu, J., Lehmann, B., Li, C., Li, G., Zhang, L., Guo, J., Sun, W., 2017b. Combined zircon and cassiterite U-Pb dating of the Piaotang granite-related tungsten-tin deposit, southern Jiangxi tungsten district, China. *Ore Geol. Rev.* 82, 268-284.
61. Zhang, S., Zhang, R., Lu, J., Ma, D., Ding, T., Gao, S., Zhang, Q., 2019a. Neoproterozoic tin mineralization in South China: geology and cassiterite U-Pb age of the Baotan tin deposit in northern Guangxi. *Miner. Depos.* 54 (8), 1125-1142.
62. Zong, K., Chen, J., Hu, Z., Liu, Y., Li, M., Fan, H., Meng, Y., 2015. In-situ U-Pb dating of uraninite by fs-LA-ICP-MS. *Sci. China Earth Sci.* 58 (10), 1731-1740.